Title

Chimpanzee and pig-tailed macaque iPSCs: Improved culture and generation of primate cross-species embryos

Journal

Cell Reports, 40(9)

ISSN

2639-1856

Authors

Roodgar, Morteza
Suchy, Fabian P
Nguyen, Lan H
et al.

Publication Date

2022-08-01

DOI

10.1016/j.celrep.2022.111264

Peer reviewed

HHS Public Access

Author manuscript

Cell Rep. Author manuscript; available in PMC 2023 April 05.

Published in final edited form as:

Cell Rep. 2022 August 30; 40(9): 111264. doi:10.1016/j.celrep.2022.111264.

Chimpanzee and pig-tailed macaque iPSCs: improved culture and generation of primate cross-species embryos

Morteza Roodgar[1,2], **Fabian P. Suchy**[2], **Lan H. Nguyen**[3], **Vivek K. Bajpai**[2,4], **Rahul Sinha**[2], **Jose G. Vilches-Moure**[5], **Kevin Van Bortle**[1], **Joydeep Bhadury**[2,10], **Ahmed Metwally**[1], **Lihua Jiang**[1], **Ruiqi Jian**[1], **Rosaria Chiang**[1], **Angelos Oikonomopoulos**[6], **Joseph C. Wu**[6], **Irving L. Weissman**[2], **Joseph L. Mankowski**[7], **Susan Holmes**[8], **Kyle M. Loh**[2,11], **Hiromitsu Nakauchi**[1,2], **Catherine A. VandeVoort**[9], **Michael P. Snyder**[1]

[1]Department of Genetics, Stanford University, Stanford, California, 94305, USA.

[2]Institute for Stem Cell Biology and Regenerative Medicine, Stanford University School of Medicine, Stanford, California, 94305, USA.

[3]Institute for Computational and Mathematical Engineering, Stanford University, Stanford, CA, 94305, USA.

[4]Department of Chemical and Systems Biology, Stanford University, Stanford, California, 94305, USA

[5]Department of Comparative Medicine, Stanford University, Stanford, California, 94305, USA.

[6]Stanford Cardiovascular Institute, Stanford University School of Medicine, Stanford, California, 94305, USA.

[7]Department of Molecular and Comparative Pathobiology, Johns Hopkins University School of Medicine, Baltimore, MD, 21205, USA.

[8]Department of Statistics, Stanford University, Stanford, CA, 94305, USA.

[9]California National Primate Research Center and Department of Obstetrics and Gynecology, University of California, Davis, CA, USA.

[10]Institute of Biomedicine, Sahlgrenska University Hospital, University of Gothenburg, SE 413 45, Gothenburg, Sweden.

[11]Department of Developmental Biology, Stanford University School of Medicine, Stanford, California, 94305, USA.

Summary

Corresponding authors: mpsnyder@stanford.edu, cavandevoort@ucdavis.edu, nakauchi@stanford.edu.
Lead Contact: mpsnyder@stanford.edu

Author contribution: MR conceived the study, species selection, iPSC derivation, and NHP iPSC media optimization. KML guided on iPSC medium optimization. MR and FPS conducted iPSC fluorescent-labeling, single cell expansion and *BCL2* transduction. CAV conducted rhesus macaque oocyte retrieval, IVF, and embryo generation. FPS conducted embryo injection and imaging. MR, FPS, JB conducted iPSC co-culture experiments. MR, VKB, and AO conducted cardiomyocyte differentiation and evaluation. MR, LHN, RC, KVB, and RS conducted transcriptome experiments and analysis. LH, RJ, AM, and MR conducted proteomics experiments and analysis. MR, LHN, AM, and RS conducted transcriptome and proteomics analysis. VKB conduced ectoderm differentiation. MR and JGVM conducted *BCL2* teratoma assays and histopathology analysis. JLM supervised species selection. KVB and JLM edited the manuscript. JCW supervised cardiomyocyte experiments. CAV, HN, and MPS supervised the study.

As our closest living relatives, non-human primates uniquely enable explorations of human health, disease, development, and evolution. Considerable effort has thus been devoted to generating induced pluripotent stem cells (iPSCs) from multiple non-human primate species. Here we establish improved culture methods for chimpanzee (*Pan troglodytes*) and pig-tailed macaque (*Macaca nemestrina*) iPSCs. Such iPSCs spontaneously differentiate in conventional culture conditions, but can be readily propagated by inhibiting endogenous WNT signaling. Chimpanzee and pig-tailed macaque iPSCs cultured in these enhanced conditions can differentiate into cardiomyocytes and neural crest *in vitro* and form teratomas *in vivo*. As a unique functional test of these iPSCs, we injected them into the pre-implantation embryos of another non-human species, rhesus macaques (*Macaca mulatta*). Ectopic expression of anti-apoptotic gene *BCL2* enhances the survival and proliferation of chimpanzee and pig-tailed macaque iPSCs within the pre-implantation embryo, although the identity and long-term contribution of the transplanted cells warrants further investigation. In summary, we disclose transcriptomic, cell lines, and cell culture resources that may be broadly enabling for non-human primate iPSC research.

Graphical Abstract

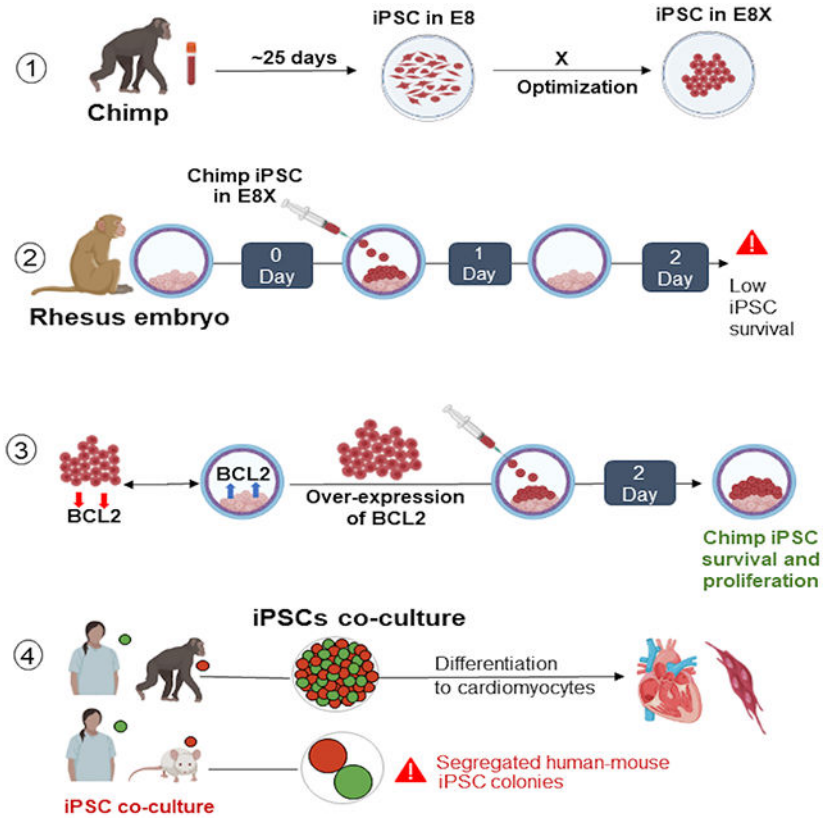

Introduction

Non-human primates are our closest living relatives. By virtue of their genetic, anatomical, and physiological similarities to humans, non-human primates afford unique opportunities to explore aspects of human health, disease, development, and evolution that would otherwise

prove challenging to explore in more evolutionarily-diverged model organisms. Here our experiments focus on 3 non-human primate species—chimpanzee (*Pan troglodytes*), pig-tailed macaque (*Macaca nemestrina*), and rhesus macaque (*Macaca mulatta*)—that have diverged across ~25 million years of evolution (Gibbs et al., 2007).

The importance of non-human primates in basic and translational research has galvanized efforts to produce induced pluripotent stem cells (iPSCs) from a variety of primate species, including chimpanzee, rhesus macaque, pig-tailed macaque, Japanese macaque, marmoset, bonobo, gorilla, and orangutan (Navara et al., 2013, Romero et al., 2015, Zhong et al., 2011, Nakai et al., 2018, Wu et al., 2010). The forced overexpression of various transcription factors can dedifferentiate mature cells into iPSCs, which are pluripotent and can theoretically generate any cell-type within the body. Therefore, the generation and propagation of non-human primate iPSCs unlocks the possibility of generating desired cell-types from a given species.

However, culture conditions for non-human primate iPSCs are generally less well-established by comparison to human iPSCs. Decades of work have established that the two principal extracellular signals that maintain human iPSCs in a primed, pluripotent state are TGFβ and FGF (Vallier et al., 2005, Bendall et al., 2007, Mossahebi-Mohammadi et al., 2020), which are the basis for the widely-used mTeSR1 and E8 culture media for human iPSCs (Chen et al., 2011a). However, we noted that conventional culture media optimized for human iPSC propagation was not ideal for non-human primate iPSCs, which tended to spontaneously differentiate in such conditions. Past work with mouse and human pluripotent stem cells showed that they endogenously produce WNT ligands, which trigger spontaneous differentiation into primitive streak cells (Blauwkamp et al., 2012, Gadue et al., 2006). We thus hypothesized that inhibition of WNT signaling might stabilize non-human primate iPSCs and avert spontaneous differentiation.

Here we establish enhanced culture conditions for pig-tailed macaque and chimpanzee iPSCs, relying on the pharmacologic blockade of WNT signaling. Chimpanzee and pig-tailed macaque iPSCs cultured in these enhanced conditions can differentiate into cardiomyocytes and neural crest *in vitro* and form teratomas *in vivo*. Finally, we demonstrate that pig-tailed macaque and chimpanzee iPSCs are capable of survival and proliferation upon injection into blastocysts of another non-human primate species (rhesus macaques), although the identity and long-term of the transplanted cells awaits further investigation. These improved methods to propagate non-human primate iPSCs while retaining important functional hallmarks of such cells should enrich the non-human primate iPSC toolkit, with ramifications for myriad applications.

Results

Improved culture of chimpanzee and pig-tailed macaque iPSCs

We derived iPSCs from two NHP species, chimpanzee (*Pan troglodytes*) and pig-tailed macaque (*Macaca nemestrina*), and transplanted them into blastocysts isolated from a third NHP species, rhesus macaque (*Macaca mulatta*) (Figure 1A). Phylogenetic comparisons illustrate that these three NHP species have diverged across ~25 million years (Figure 1A).

To establish chimpanzee and pig-tailed macaque iPSCs, we reprogrammed peripheral blood mononuclear cells (PBMCs) from these respective species by transducing them with Sendai viruses encoding *OCT4/POU5F1*, *SOX2*, *KLF4* and *C-MYC* (Takahashi et al., 2007, Fusaki et al., 2009, Ban et al., 2011) and validated iPSCs normal karyotypes (Supplementary Figure S1A & S1B). However, chimpanzee and pig-tailed macaque iPSCs spontaneously differentiated when cultured in E8 medium (Figure 1B & Supplementary Figure S1C), which was originally optimized for the propagation of human primed PSCs (Chen et al., 2011b, Wu et al., 2015). Given past work that primed PSCs endogenously produce WNT ligands, which trigger primitive streak differentiation, we hypothesized that inhibition of WNT signaling using the small molecule XAV939 ((Huang et al., 2009); "E8X") might reduce spontaneous differentiation in NHP iPSCs, analogous to results in human and mouse primed PSCs (Wu et al., 2015). Compared to E8 medium, the use of E8X reduced spontaneous differentiation of NHP iPSCs, increasing the percentage of $OCT4^+$ cells, while preserving their normal karyotype (Supplementary Figure S1B, S1C & S1F). In E8X media, chimpanzee iPSCs could be maintained in feeder-free conditions (on recombinant laminin-511 coated plates), whereas pig-tailed macaque iPSCs were cultured on mouse embryonic fibroblasts (MEFs) in E8X medium (Figure 1B). In these optimized E8X culture conditions, both chimpanzee and pig-tailed macaque iPSCs could form teratomas *in vivo* ("teratoma assay") in NSG mice (Supplementary Figure S1E) and could differentiate into cranial neural crest cells *in vitro* (Supplementary Figure S1D). Taken together, inhibition of endogenous WNT signaling enhances the propagation of both the chimpanzee and pig-tailed macaque iPSCs, while preserving the pluripotency and genomic integrity of such cells.

Limited survival of chimpanzee and pig-tailed macaque iPSCs injected into rhesus pre-implantation embryos

Following the establishment of optimized chimpanzee and pig-tailed iPSCs, we evaluated whether iPSCs injected into rhesus macaque early blastocysts can survive and proliferate 48 hours post injection. Oocyte retrieval from rhesus macaques was performed by ultrasound-guided aspiration of follicles that occurred roughly 33 hours following hCG administration. Oocyte fertilization and embryo culture were performed according to our standard in vitro protocols (see methods) (VandeVoort et al., 2009, De Prada and VandeVoort, 2008). We injected 8-12 iPSC donor cells into each rhesus macaque early blastocyst. Using the expression of td-Tomato red fluorescent protein as an iPSC-specific marker, we evaluated the survival of injected iPSCs via imaging 2 days after injection into the rhesus blastocyst (Figure 1D). While our preliminary results indicated that chimpanzee iPSCs could survive 48 hours post injection (Figure 1D), this success was achieved at very low efficiency (3 embryos survived and 1 showed evidence of iPSCs survival). Moreover, the robustness of iPSC survival and proliferation was fairly limited based on td-Tomato expression marker levels within the rhesus embryoblast (Figure 1D-E). We observed that pig-tailed macaque iPSCs, on the other hand, survived and aggregated near rhesus ICM in at an improved efficiency (6 out of 11 developed embryos), potentially driven by the close evolutionary distance between pig-tailed macaque and rhesus macaque (Figure 1A, E).

The survival of iPSCs within the blastocyst of rhesus macaque 48 hours post injection represents a significant first step towards cross-species chimera formation. However,

although the numbers are small, the low efficiency and survival of chimpanzee iPSCs in rhesus embryos presents a significant challenge for downstream experiments, as embryo injection experiments are limited by the low-throughput and limited seasonal nature of oocyte retrieval during reproductive cycles (November-February) of rhesus macaques (Dailey and Neill, 1981, Riesen et al., 1971).

Comparative analysis of transcript abundance identifies molecular signatures of the rhesus embryoblast, including core pluripotency factors and *BCL2*

To improve iPSCs quality before injection into pre-implantation embryos, we first sought to better understand the molecular signatures of the rhesus ICM and expression of genes involved in cell survival during early embryonic development by comparing the transcriptome profiles within the rhesus macaque ICM with the optimized pig-tailed and chimpanzee iPSCs. The limited cell quantity within the Inner Cell Mass presents a challenge for typical genomic approaches. With this in mind, we applied a low-input RNA-sequencing strategy to both rhesus ICM and appropriately matched iPSC numbers (approximately 40-50 chimpanzee or pig-tailed iPSCs). For broader comparison groups, we additionally isolated mouse blastocyst ICM and iPSCs derived from humans. We processed, pooled, and sequenced all samples concurrently to avoid batch effects and variation introduced during sample processing. We used principal component analysis (PCA) to broadly compare the transcript abundances across all cell types. Transcript abundance patterns cluster by cell types/stages as well as species donor and host material. We observed separation of ICMs and pluripotent stem cells (PSCs) along the first principal component (PC1) in the gene expression data (PC1= 48.5%; Figure 2A). Among the PSCs, principal components 2 (PC2) and 3 (PC3) appear to be driven by species (PC2 = 13.4%; Figure 2A), as we observe all rhesus macaque samples clustering together despite their different cell types (PC3= 9.6%; Supplementary Figure S2A). A list of the top 100 genes contributing to PC1 and PC2 are provided in Supplementary Figures S2H and S2I, respectively. Genes segregating human and primate PSCs include higher expression of *NDUFA13*, *RPS15A*, *RPL38*, *MT-CYB* in human iPSCs (Supplementary Figure S2G). Altogether, the principal component analysis indicates that the expression profiles captured by low-input RNA-sequencing are appropriately driven by the developmental context and species from which the iPSCs and ICM were derived.

Comparative analysis of transcript abundance between NHP iPSCs and the rhesus ICM identifies significantly differential expressed genes, including 1,173 (chimpanzee iPSC v. rhesus ICM; FDR < 0.05) and 4,838 (pig-tailed macaque iPSC v. rhesus ICM; FDR < 0.05) genes up- or down-regulated more than 2 fold (Figures 2B-C). Among the significantly differential genes, several core pluripotency factors, such as *KLF4*, *VIM*, and *MBD3,* that have been shown to play essential roles in pluripotency and chimera formation, exhibited an intrinsically higher expression in rhesus ICM compared to the iPSCs (Figure 2B-C) (Dunn et al., 2014, Masaki et al., 2016, Takahashi et al., 2007, Takashima et al., 2014, Theunissen et al., 2014, Gafni et al., 2013, Martello and Smith, 2014, Stirparo et al., 2018). These results are consistent in chimpanzee, pig-tailed macaque, and Human iPSCs in comparison to rhesus ICM, suggesting the expression of these core pluripotency factors is likely to play an important role during early stages of development.

To better understand the pluripotency potential of the different primate iPSCs and rhesus ICM, we examined the expression profile of pluripotency markers and related genes connected through biological interaction. A gene interaction network between chimpanzee and pig-tailed iPSCs and the rhesus macaque ICM was generated using the String database, (STRING v11) (Szklarczyk et al., 2019, Hall et al., 2009, Dunn et al., 2014, Martello et al., 2012, Martello et al., 2013, Niwa et al., 2009, Qiu et al., 2015, Tai and Ying, 2013, Yang et al., 2010, Yeo et al., 2014, Yuri et al., 2009, Savatier et al., 2017, Stirparo et al., 2018, Boroviak et al., 2018, Yamane et al., 2005, Liu et al., 2021) and the a qualitative assessment of the gene network revealed significantly lower expression of *BCL2* in chimpanzee and pig-tailed macaque iPSCs compared to rhesus ICM (Supplemental Figures 2D-E). This result highlights a potentially critical role of *BCL2* expression in rhesus ICM suggesting that *BCL2* may play an important role in cell survival within the early developmental environment of the ICM.

Ectopic *BCL2* expression in NHP iPSCs improves efficiency of cross-species blastocyst chimera formation ex-vivo

Our finding that *BCL2* is expressed in the rhesus ICM led us to speculate that *BCL2* may be important for cell survival during early development, and that ectopic expression of *BCL2* may improve the survival of iPSCs, thereby increasing the success rate of cross-species chimerism. Indeed, previous reports indicate that *BCL2* expression improves chimera formation in rodent species (Masaki et al., 2016). To test whether ectopic *BCL2* expression improves the survival of chimpanzee and pig-tailed macaque iPSC donor cells, we injected iPSCs stably transfected with a *BCL2* overexpression construct into rhesus macaque embryos (Figures 3A & 3B). The *BCL2* overexpression construct contains a CAG promoter that allows for constitutive expression of *BCL2* in the transfected iPSCs and includes a neomycin resistance gene for selection of transfected iPSCs. The iPSCs were treated with neomycin for 3 passages post transfection with the *BCL2* vector to select for transfected iPSCs (see method). *BCL2* was shown to be expressed in the transfected iPSCs of both chimpanzee and pig-tailed macaque (Supplementary Figure S3A). Ectopic expression of *BCL2* did not cause chromosomal abnormalities in iPSCs as evaluated by chromosomal karyotype (Supplementary Figure S3B). Additionally, despite a significant range in the level of overexpression of *BCL2* in iPSCs at the RNA level, analysis of protein abundance in iPSCs with and without *BCL2* overexpression identifies a 2-4 fold increase in *BCL2* abundance, with otherwise limited changes in the proteome of iPSCs (Supplementary Figure S3C).

Approximately 8-12 chimpanzee or pig-tailed macaque red-fluorescent-tagged iPSCs were injected into 99 rhesus embryos (chimpanzee n=59; pig-tailed n=40). Two days after injection, 22 out of 23 (95.6%) rhesus embryos injected with chimpanzee *BCL2*-expressing iPSCs survived; chimpanzee iPSCs proliferated inside the rhesus macaque embryos near the ICM, as indicated by expanded red florescent areas in the embryos (Figure 3A). Similar results were observed after injection of the *BCL2*-expressing pig-tailed macaque iPSCs for which all of 10 (100%) of injected embryos survived (Figure 3B). In contrast, most of the control iPSCs without *BCL2* overexpression did not survive in rhesus blastocysts during this time period (33.3% chimpanzee; 54.5% pig-tailed macaque Figures 3C & 3D) (Table 1).

Estimation of the number of tdTomato positive cells provides evidence that injected iPSCs expanded in number within the rhesus macaque embryos (Figure 3E). Time-lapse video imaging of the injected rhesus macaque embryos further captures the expansion of iPSCs and their migration towards the rhesus ICM (Supplementary Video 1). These results indicate that the injected cells survived, proliferated and integrated into rhesus macaque ICM, with a significant improvement in success rate and robustness compared to iPSCs without *BCL2* expression. Additionally, we observed some of the *BCL2*-expressing chimpanzee iPSCs migrated to the trophectoderm area of rhesus blastocysts. (Supplementary Figure S3E and Supplementary Video 1). These results suggest nonhuman primate blastocyst chimeras can be generated with high efficiency. and *BCL2* may provide a critical tool for chimera formation and personalized organ development.

Ectopic *BCL2* expression in NHP iPSCs does not interfere with differentiation potential in a mouse teratoma model

Because *BCL2* expression significantly enhanced cross-species chimerism for NHP donor iPSCs, we next sought to determine whether *BCL2* expression interferes with the differentiation potential of these stem cells, as this would effectively limit the utility of *BCL2* in downstream development experiments. Using a mouse teratoma model, we tested whether *BCL2*-overexpressing iPSCs formed all three germ layers (ectoderm, mesoderm and endoderm) similar to non-*BCL2* transduced iPSCs (see methods for the assays). As expected, teratomas developed from chimpanzee iPSCs and pig-tailed macaque iPSCs with and without *BCL2* in the testes and subcutaneous tissues of NSG mice (Supplementary Figure S4A & S4B). The changes in the size of the tumor in each mouse were recorded every 3 days and tumor growth was measured. Importantly, growth rates of teratomas formed from iPSCs with or without ectopic *BCL2* expression were similar (Supplementary Figure S4C & S4D). At the completion of the teratoma study, tissues from the NSG mice were thoroughly examined histologically. Tissues examined include dorsal haired skin, reproductive tract, liver, gallbladder, spleen, kidneys, adrenal glands, pancreas, salivary gland, mandibular lymph nodes, heart, lung, trachea, esophagus, tongue, eyes, brain, and cerebellum. There was no evidence of metastasis nor any other abnormality in any of the examined tissues (Supplementary Table 1). Differentiated cells were observed independent of *BCL2* transduction (Supplementary Figure S4A & S4B). Similar results were also found using the human H9 cell line and *BCL2*-expressing H9 cell line (Supplementary Figure S4E). Additionally, staining of POU5F1 in teratoma tissues did not identify any cells immunopositive for POU5F1, indicating that no iPSCs expressing *BCL2* are left undifferentiated (Supplementary Figure S4F-H). These results indicate that expression of *BCL2* in primate pluripotent stem cells does not interfere with the differentiation potential of these cells, suggesting ectopic expression of *BCL2* may be utilized for future downstream developmental experiments and blastocyst complementation related organ generation.

Chimpanzee iPSCs co-culture and co-differentiate with Human iPSCs, suggesting chimpanzee iPSCs are an ideal surrogate model system for Human-related studies

Given the phylogenetic comparison of nonhuman primates and evolutionary distance between humans and chimpanzee, we further queried the ability of chimpanzee iPSCs to serve as a surrogate model system for humans, given the technical and ethical concerns of

cross-species chimerism in humans. Specifically, we tested the functional and developmental similarities of chimpanzee and human iPSCs in an *in vitro* culture setting by co-culturing human and chimpanzee iPSCs and differentiating them into cardiomyocytes. We mixed equal number of single-cell dissociated human and chimpanzee iPSCs and seeded ~40,000 total cells on plates coated with iMatrix-511 (Figure 4A). Co-culturing human and chimpanzee iPSCs indicated that the two cell types do not form distinct and separate iPSC colonies and mixed homogenously in a blended manner similar to that of co-culturing two different human iPSC cell lines (Figure 4A). In contrast, co-culture of human iPSCs and mouse EpiSCs resulted in separate, distinct colonies (Figure 4A). Thus, chimpanzee and human iPSCs appear functionally similar *in vitro*. We next differentiated the mixture of human and chimpanzee iPSCs into cardiomyocytes following existing protocols for human iPSC differentiation (method section) (Lian et al., 2012, Lian et al., 2013). The mixture of human and chimpanzee differentiating iPSCs formed beating cardiomyocyte aggregates (Figure 4B, Supplementary videos 2-5). To the best of our knowledge, this is the first *in vitro* differentiation of a mixture of iPSCs from two different species. Thus, although the use of human iPSCs for embryonic cross-species chimera studies is restricted, these results demonstrate that chimpanzee iPSCs appear functionally equivalent to human iPSCs. In addition, transcript analysis of iPSCs from different species revealed that principal component 3 is driven by species and that human and chimpanzee iPSCs cluster together (Supplementary Figure S2A) indicating the iPSCs are similar and suggesting that chimpanzee iPSCs could serve as a surrogate for human iPSCs.

Discussion

We show that *BCL2*-overexpressing chimpanzee and pig-tailed macaque iPSCs derived in E8X media can survive and proliferate in the vicinity of the ICM when injected into rhesus macaque pre-implantation embryos. This improved condition for primate iPSCs is a necessary first step on the path to eventually generate functionally viable primate iPSCs that can form cross-species chimeras between two primate species. Future steps must entail the implantation of these iPSC-injected blastocysts into pseudopregnant primate recipients, which is technically and logistically challenging but is the *de rigueur* test of whether these iPSCs within the cross-species blastocysts can continue developing *in utero*. Our results provide a justification for pursuing such blastocyst implantation experiments into primates.

We optimized culture conditions for NHP iPSCs through the addition of XAV939, a WNT inhibitor that reduced spontaneous differentiation and thus improved the maintenance of NHP iPSCs. This is consistent with how WNT inhibition improves the propagation of primed PSCs in human, chimpanzee, rhesus macaques, and mouse (Sokol, 2011, Wu et al., 2015, Loh and Lim, 2015).

Despite these improvements, chimpanzee and pig-tailed macaque iPSCs maintained in E8X media did not robustly engraft the blastocyst of rhesus macaques. This limited blastocyst engraftment may be ascribed to the primed state of pluripotency. Mouse primed PSCs, which correspond to post-implantation pluripotent cells, fail to survive and proliferate upon injection into pre-implantation mouse blastocysts (Masaki et al., 2016, Tesar et al., 2007, Brons et al., 2007), as they are developmentally mismatched. The majority of NHP PSC

lines are in a primed pluripotent state, and this has been long viewed as an impediment to their use in generating cross-species blastocyst chimeras (Suchy and Nakauchi, 2017): indeed, rhesus macaque PSCs are unable to engraft blastocysts from the same species (Tachibana et al., 2012).

However, overexpression of the antiapoptotic gene *BCL2* been shown to enhance the engraftment of primed PSCs into recipient blastocysts (Masaki et al., 2016, Wang et al., 2018). Our transcriptomic data also revealed low expression of *BCL2* in chimpanzee iPSCs and pig-tailed macaque iPSCs relative to the rhesus macaque ICM (Figure 2B&C). Based on our transcriptome data and the previous successful use of *BCL2* in improving the engraftment of human and mouse primed PSCs into the blastocyst (Masaki et al., 2016, Wang et al., 2018), we overexpressed *BCL2* in our NHP iPSC lines. *BCL2* overexpression in chimpanzee and pig-tailed macaque iPSCs enhanced their survival and proliferation for at least 2 days upon transplantation into rhesus macaque preimplantation embryos. Moreover, the *BCL2*-overexpressing iPSCs aggregated in or around the rhesus ICM, which is the region of the blastocyst that develops into the fetus (as opposed to the placenta). The next crucial step is to implant these cross-species blastocysts into pseudopregnant primates to assess whether they can further develop *in utero*. These blastocyst implantation experiments are justified by our blastocyst engraftment findings, but are technically and logistically complex due to complexities with experimenting on non-human primates.

Thus far, most experiments to transplant primate PSCs (e.g., human PSCs) into the blastocyst have injected them into the mouse blastocyst (Theunissen et al., 2014, Takashima et al., 2014, Gafni et al., 2013). While an advantage of the mouse blastocyst model is that these blastocysts can be readily implanted into pseudopregnant mice to test whether they can develop into chimeric fetuses *in utero*, it is important to note that human and mouse have diverged across ~96 million years of evolution (Nei et al., 2001), which may underscore difficulties in generating chimeras. One pioneering study injected human PSCs into pig blastocysts, but found limited contribution to chimeras (Wu et al., 2017); this might be due to poor quality of human (primate) iPSCs or simply because of large evolutionary distance between human and pig that are estimated to have diverged ~91 million years ago (Jørgensen et al., 2005). Additionally, due to ethical concerns, injection of human iPSCs into primate embryos is limited to *in vitro* experiments only (Tan et al., 2021). Moreover, while under certain circumstances it is ethical to transplant human PSCs into rodent and pig blastocysts (Wu et al., 2016, Suchy and Nakauchi, 2017), it is currently ethically impermissible to inject them into non-human primate embryos and transplant the chimeric embryos into a female nonhuman primate recipient (Suchy and Nakauchi, 2017, Hermerén, 2015, Tan et al., 2021), and therefore we did not inject human iPSCs into the rhesus blastocysts. Instead, we injected optimized iPSCs from chimpanzees (which are the closest living ancestors to human (King and Wilson, 1975)) into rhesus macaque blastocysts. We find that chimpanzee and human iPSCs can homogeneously mix *in vitro* in both the undifferentiated and differentiated state, supporting the notion that findings with chimpanzee iPSCs can likely be extrapolated to human iPSCs. The use of chimpanzee iPSCs as a surrogate for human iPSCs is translationally important for functional validation of primate iPSCs through formation of cross-species chimeras.

We also recognize that understanding the potential of *BCL2*-overexpressing cells for post-implantation development remains an important direction for future applications of this system. While we and others have shown that *BCL2*-overexpressing human and non-human primate PSCs can still differentiate *in vivo* (forming teratomas) and *in vitro* (Ardehali et al., 2011), constitutive *BCL2* expression could have untoward effects. While *BCL2* is used to promote the survival of primed PSCs upon blastocyst injection, progress is rapidly advancing in generating naïve-like PSCs from primate species (Gafni et al., 2013, Takashima et al., 2014, Theunissen et al., 2014, Fang et al., 2014), and transplantation of such cells into the pre-implantation embryo may allow them to survive without the need for exogenous *BCL2* expression. We identified *BCL2* (intrinsically highly expressed in rhesus macaque ICM) as a critical molecular driver of survival and integration of chimpanzee and pig-tailed macaque iPSCs into the host ICM (rhesus macaque). We also identified *KLF4* (highly expressed in rhesus macaque ICM) as an additional potential driver of cross-species chimerism among primate species. The improvement in derivation of functionally viable chimpanzee and pig-tailed macaque iPSCs is important as it has long been believed that only rodent iPSCs have the pluripotency features that would allow iPSCs survival in a closely related host blastocyst and formation of closely related cross-species chimeras.

The next step is to conduct embryo transfer of rhesus macaque blastocysts (that have been transplanted with NHP iPSCs) into female rhesus macaque recipients. This will conclusively determine whether *BCL2*-expressing chimpanzee and pig-tailed macaque iPSCs can develop further *in vivo*, thus investigating the potential of cross-species chimera formation among nonhuman primate species. These studies using chimpanzee iPSCs are anticipated to serve as a useful model for future studies of human and other primates regenerative medicine.

RESOURCE AVAILABILITY

Lead Contact

Further information and request for resources and reagents should be directed to and will be fulfilled by the Lead Contact, Michael P. Snyder (mpsnyder@stanford.edu).

Materials Availability

The new chimpanzee and pig-tailed macaque iPSC lines are available from the lead contact upon request and preparing Material Transfer Agreement (MTA). The cell lines will also be deposited in a public repository.

Data and Code Availability

Data—Data have been deposited at NCBI GEO and are publicly available as of the date of publication. Accession numbers are listed in the key resources table.

Code Availability—This paper does not report original code.

- Any additional information required to reanalyze the data reported in this paper is available from the lead contact upon request.

EXPERIMENTAL MODEL AND SUBJECT DETAILS

Animal care and use

All animals used in this study were treated following the Institutional Animal Care and Use Committee (IACUC) protocol at University of California Davis, and Administrative Panel on Laboratory Animal Care (APLAC) protocol at Stanford University, Stem Cell Research Oversight (SCRO) at Stanford University and Administrative Panel on Biosafety (APB) protocol at Stanford University.

Peripheral blood mononuclear cells (PBMCs) from a 14-year-old male pig-tailed macaque (*macaca nemestrina*) and an 11-year-old female chimpanzee (*Pan troglodytes*) were used to generate new iPSCs.

METHOD DETAILS

iPSCs derivation and maintenance

Chimpanzee (Pan troglodytes) iPSCs—Chimpanzee peripheral blood mononuclear cells (PMBCs) were obtained from Southwest National Primate Research Center (SNPRC), San Antonio, Texas, USA according to the corresponding SNPRC IACUC protocol. and the PBMCs were reprogrammed into induced pluripotent stem cells (iPSCs) optimizing a feeder free condition(Ohmine et al., 2011). In summary, PBMCs were cultured to expand blood progenitor cells in Stem Span medium (Stemcell Technologies Inc. Vancouver, Canada) for 9 days. The next day (day of reprogramming, “day 0”), the cells were transfected with Sendai virus with four transcription factors including c-myc, KLF4, SOX2, OCT3/4 using CytoTune 2.0 kit (ThermoFisher Scientific, Waltham, MA, USA). On the day after transfection (day 1), all the cells transfected with Sendai virus were transferred into the plates coated with Matrigel Matrix (Corning Inc., Corning, NY, USA) in StemSpan medium (Stemcell Technologies Inc. Vancouver, Canada). On day 2, floating cells were transferred to new wells of a Matrigel-coated 6-well plate in 2 mL of Stem Span medium. On day 3, 2ml of Essential-6 medium (E6) (ThermoFisher Scientific, Waltham, MA, USA) were added into existing 2mL StemSpan medium and cells in the 6-well plates, and the mixture was left unchanged on day 4. On day 5, the media in each well was removed and replaced by 2mL of E6 medium and left unchanged on day 6. On day 7, all medium was removed and 2mL of E6 medium + 100 ng/mL of bFGF (ThermoFisher Scientific, Waltham, MA, USA) were added. On days 8, 9, and 10 the medium was replaced with 2mL E7 (Essential 6 medium + 100ng/ul of FGF). Starting on day 11, the medium was replaced by E8 (Chen et al., 2011c) until days 16 to day 18 when the first colonies of iPSCs were observed. Each colony was manually picked with 1000μL pipet and was cultured on new Matrigel-coated plates in E8 medium with 2μM of Thiazovivin (TZV) on the first day after passage. After the first passage, 2nM of Wnt inhibitor (XAV939) were added to the E8 medium which resulted in colonies with little-to-no differentiation. For the subsequent passaging, the wells were coated with 5μL of iMatrix-511 (Takara Bio Inc. Kusatsu, Japan) in 2mL of the E8 + E8 specific supplement + XAV939 (2nM) for expansion.

Pig-tailed macaque (Macaca nemestrina) iPSCs—Blood samples were obtained from a 12-year old male pig-tailed macaque from the Johns Hopkins University colony. The PBMC (peripheral blood mononuclear cells) were isolated from whole blood in each sample and were then reprogrammed into induced pluripotent stem cells (iPSCs) making modifications and optimizing a previously published feeder free protocol(Ohmine et al., 2011). In summary, PBMCs were cultured in medium to expand blood progenitor cells in StemSpan medium for 9 days. The next day, the cells were transfected with Sendai virus of four transcription factors c-myc, KLf4, Sox2, Oct3/4 using CytoTune 2.0 kit (ThermoFisher, Waltham, MA, USA) on the day of reprogramming (day 0). On the day after transfection (day 1), all the cells transfected with Sendai virus were transferred into a 6-well plate (30,000 cells per well) each well containing ~150,000 mouse embryonic fibroblast (MEF) feeder cells (Stemcell Technologies Inc. Vancouver, Canada). The MEF plate preparation was conducted the day before plating the reprogramming cells as explained elsewhere (Takahashi et al., 2007). On day 2, the floating cells were transferred to new wells of 6-well plate containing MEF in 2 mL of the Stem Span media. On day 3, 2mL of in Essential-6 media (ThermoFisher Scientific, Waltham, MA, USA) were added into existing 2mL StemSpan medium on MEF in which transfected cells were. No medium change on day 4 was conducted. On day 5, all the medium in each well were removed and replaced by E6 medium. No medium change on day 6 was conducted. On day 7, all medium was removed and 2mL of E6 + 100 ng/mL of bFGF (Stemcell Technologies Inc. Vancouver, Canada) were added. On day 8, 9, and 10 media was changed and with E7 (E6 + 100ng/ul of FGF). From day 11, the media was replaced by E8 until days 16 to day 18 when the first colonies of iPSC were observed. Each colony was manually picked with 1000μL pipet and were cultured on new matrigel-coated plated in E8 media and 2μM of TZV on the first day after passage. After the first passage, 2nM of Wnt inhibitor (XAV939) were added into the E8 media which resulted in colonies with little-to-no differentiation. For subsequent passaging and expansion, the iPSCs were washed with PBS and were incubated at using 1mL of Accumax (Stemcell Technologies Inc. Vancouver, Canada) for one well of a 6-well plate for 5 minutes at 37°C. The Cells were then aspirated, and single cell dissociated using a 1000μL. The cells were suspended in E8X medium with 2μM of TZV on mouse embryonic fibroblast cells (MEF) for each passaging during the expansion and maintenance.

iPSCs Karyotyping: The chimpanzee and macaque-derived (*Macaca nemestrina*) cell lines were harvested by standard cytogenetic methodology of mitotic arrest, hypotonic shock and fixation with 3:1 methanol-acetic acid. Chromosome slide preparations were stained by G-banding and classified by the standard ***P. troglodytes*** *and M. nemestrina* karyotype 1, 2. Analysis of 20 metaphase of pig-tailed macaque cells demonstrated an apparently normal male karyotype of 20 autosomes and two sex chromosome (XY) in all cells (Brown et al., 1986, O'Brien et al., 2006). Additionally, chimpanzee iPSCs either with or without *BCL2* transfection demonstrated and apparently normal male chromosomes karyotype.

iPSCs labeling with fluorescent vector and Bcl2 vector: The iPSC from chimpanzee and pig-tailed macaque were transfected with the td-Tomato (tdT) red fluorescent vector (Masaki et al., 2016). The tdT transfected cells were then clonally expanded from single cells to make sure all the cells from each clone contained the same number of td-Tomato genes.

This was done to minimize the heterogeneity in expression of tdTomato among iPSC. The tdTomato single cells expanded iPSC were subsequently transfected with the *BCL2* vector containing neomycin resistance gene(Masaki et al., 2016). The iPSCs then were expanded clonally from single cells and treated with neomycin for two weeks to obtain iPSCs with same number of integrated *BCL2* in each cell. The iPSCs containing tdT and *BCL2* were then used for the injection into rhesus macaque embryos.

Alkaline Phosphatase (AP) Stain.: Cells were rinsed twice with DPBS and fixed for five minutes at room temperature (RT) with 4% PFA. Then 1-Step™ NBT/BCIP Substrate Solution (Cat No. #34042, ThermoFisher Scientific, USA) was added to the wells and allowed to develop for 8-10minutes at RT. The solution was aspirated and the wells were washed twice with DPBS before being imaged.

Co-culture experiment of iPSCs.: Equal numbers iPSCs from each species was used for the paired species co-culture experiment. The paired iPSCs from human and chimpanzee, human and human, human and mouse, and mouse and mouse (40,000 cells from each species) were cultured to perform co-culture experiments. The differentiation into cardiomyocytes was conducted on these co-cultured cells as described in iPSCs into cardiomyocyte differentiation section (below).

Teratoma assay.: The iPSCs were cultured and dissociated using Accumax (Stemcell technologies Inc. Vancouver, Canada) in E8 + supplement and XAV939 (2nM) and TZV (2μM). The cells were washed once with E8 + supplement and XAV939 (2nM) and TZV (2μM) media (75%) and 25% DMEM-F12 in total concentration 70 million cells /mL. 30μL of the solution containing total of 2.1 million cells (or placebo controls) were injected subcutaneously on the dorsum of each mouse. The same number of cells were injected into the testes. Tumors were monitored and tumor size was measured, every other day for 60 days.

Histopathology.: At the end of the study, mice were humanely euthanized via CO_2 inhalation. Tissues were assessed for gross evidence of tumor burden, and tissues were collected in 10% neutral buffered formalin (NBF). After fixation, tissues were routinely processed, paraffin embedded, sectioned at 5.0μm, and sections routinely stained with hematoxylin and eosin (H&E). Tissue sections were examined for the presence of teratomas. Teratomas were defined as tumors of embryonic origin containing the three embryonic germ layers (endoderm, mesoderm, ectoderm) and/or their derivatives. When present, teratomas were assessed for evidence of malignant transformation such as local invasion into the adjacent tissues. Histologic assessment was performed using an Olympus BX43 upright brightfield microscope, and images were captured using the Olympus cellSens software.

qPCR.: qPCR for pluripotency markers were conducted using the conserved probes designed to work for a wide range of primate species including both human and rhesus macaque. A list of all pluripotency genes measured via qPCR and the corresponding primers and probes are listed in supplementary table (Supplementary Table 1)

Rhesus macaque oocyte retrieval, fertilization and embryo culture.

The Controlled Ovarian Stimulation (COS) protocol overrides follicle selection, resulting in numerous preovulatory follicles that respond to a timed injection of hCG to simulate the natural LH surge. One adult female rhesus monkey was used for oocyte retrieval and was housed at the California National Primate Research Center (CNPRC) in accordance with the ethics guidelines established and approved by the Institutional Animal Use and Care Administrative Advisory Committee at the University of California-Davis (Vandevoort et al., 2011). Antide (Ares-Serono, 0.5 ng /kg body weight subcutaneous) was given on the days when females were receiving FSH injections to prevent spontaneous ovulation. The COS cycle began within four days of menses as described previously with twice-daily injections of human recombinant FSH (37.5 IU) for seven days followed by a single hCG injection (1,000 IU) (VandeVoort and Tarantal, 1991, VandeVoort and Tarantal, 2001) on day 8. The volume of Antide, FSH and hCG injection vary, but in all cases were less than 1 ml. Follicle retrieval was performed by ultrasound-guided aspiration of follicles that occurred approximately 40 hours following hCG administration. All animals were allowed to have one full menstrual cycle with no interventions before another stimulation cycle is attempted. We have shown in cycles following the menstrual cycle in which thus procedure is performed, monkeys have conceived and the pregnancy uneventfully to term with normal infants, further indicating no adverse outcomes. Approximately 3cc blood sample were obtained from a peripheral vessel at the time of the aspiration (after anesthesia) and two weeks after aspiration to check for antibody to FSH and hCG per CNPRC SOP GG05. Oocyte insemination and embryo culture were performed according to our standard in vitro protocols(De Prada and VandeVoort, 2008, VandeVoort et al., 2009). Approximately 5 days after insemination, embryos were transported from CNPRC to Stanford using a portable incubator that has been shown to maintain embryo viability(Schramm et al., 2003).

Injection of NHP iPSC into the rhesus macaque embryos and imaging.

In preparation for microinjection, the pig-tailed macaque and/or chimpanzee iPSCs were dissociated to single-cells, resuspended in iPSC culture medium supplemented with 2 μM of TZV, and keep on ice. After transportation (~2-3 hours in portable incubator), the E5 rhesus macaque blastocysts were transferred to warm M2 medium (CosmoBio, Carlsbad, USA) under a microscope. A piezo-driven micromanipulator (Prime Tech, Tokyo, Japan) was used to drill through the zona pellucida and trophectoderm, after which approximately 10 iPSCs were introduced into the blastocoel. The embryos were then washed 3 times in embryo media (see Rhesus macaque oocyte retrieval, fertilization and embryo culture), after which they were placed in a 70 μL drop containing a 1:1 ratio of embryo media and N2B27 basal media (Takashima et al., 2014). Images were captured with Operetta (PerkinElmer, USA). The td-Tomato (tdT) red fluorescent area within the embryos at day 0 (the day of iPSCs injection) and day 2 (two days post injection of iPSCs) were manually defined by drawing a polygon using KLayout software. The area of polygons were calculated using Matlab and the expansion of red-fluorescent area was used as an indirect measure of iPSCs proliferation within the embryos. We also considered the aggregation of red pixels within 10 microns of ICM defined in the image near the dense ICM. The ICM was indicated using arrows in the Figures 1 and 3.

Differentiation of iPSC into cardiomyocytes.

iPSCs were differentiated into iPSC derived cardiomyocytes (iPSC-CMs) using a 2D monolayer differentiation protocol and were maintained in a 5% CO_2/air environment(Lian et al., 2012, Lian et al., 2013). Briefly, iPSC colonies were dissociated with 0.5 mM EDTA (Gibco) into single-cell suspension and re-suspended in E8 media containing 10 μM Rho-associated protein kinase inhibitor (Sigma). Approximately 100,000 cells were re-plated into Matrigel-coated 6-well plates. iPSCs were next cultured to 80-90% cell confluence, and then treated for 2 days with 6 μM CHIR99021 (Selleck Chemicals) in RPMI/B27 supplement without insulin to activate WNT signaling and induce mesodermal differentiation. On day 2, CHIR99021 was removed and cells were cultured in RPMI/B27 medium in the absence of insulin(Lian et al., 2013). On day 3, cells were treated with 5 μM IWR-1 (Sigma) to inhibit WNT pathway signaling and further promote cardiogenesis. On day 7, IWR-1 was removed from the medium and cells were placed in RPMI/B27 in the absence of insulin. From day 7 onwards, cells were placed on RPMI+B27 supplemented with insulin until beating was observed. At this point, cells were treated in starvation medium (RPMI/B27 in the absence of insulin and glucose) for 3 days. Following purification via starvation medium, the survived cells were cultured in RPMI/B27 supplemented with insulin. Starvation was repeated at day 20 for a period of three days. When re-plating iPSC-CMs for downstream use, cells were dissociated with 10X TrypLE (Life Technologies) into a single-cell suspension and seeded on Matrigel-coated plates.

RNA-seq of ICM and iPSCs

The rhesus macaque blastocysts on day 5 post IVF was used for immunosurgery to remove zonae pellucidae and trophectoderm as explained elsewhere(Mitalipov et al., 2006). In summary, the zonae pellucidae of rhesus blastocysts will be removed by exposure to 0.5% pronase in TH3 medium for 45 seconds. For immunosurgical isolation of rhesus ICM to remove trophectoderm, zona pellucidae-free rhesus blastocysts were exposed to rabbit anti-rhesus spleen serum for 30 minutes at 37°C from VandeVoort laboratory at UC Davis. Subsequently, the blastocysts were washed in TH3 medium for 3 times and were incubated in guinea pig complement reconstituted with HECM-9 (1:2 vol/vol) at 37°C for 30 minutes(Mitalipov et al., 2006). After the incubation, the trophectoderm was removed mechanically using a small-bore pipette (125μM inner diameter) and the clumps of ICM cells from each blastocyst were washed in PBS and placed in a separate PCR tube containing 5μL of RNAse-free water with 5% RNAse inhibitor. The ICMs were quickly frozen on dry ice and were stored at −80°C for cDNA synthesis and RNA-seq library preparation. The cDNA synthesis and RNA-seq were conducted directly from ICM cells using SMART-Seq V4 Ultra Low input cDNA synthesis kit (Clonetech Inc.). The cDNA concentration was measured using Quibit kit and Bioanalyzer High-Sensitivity DNA kit (Agilent Inc.). The cDNA from each ICM were used for library preparation following Illumina Nextera XT kit protocol (Illumina Inc.). The quality and the quantity of the final library were evaluated using Bioanalyzer High-Sensitivity DNA kit (Agilent Inc.),Kappa kit, and the Agilent 2100 Bioanalyzer instrument. Dual index RNA-seq library from ICMs were pooled together with dual index RNAseq libraries of approximately 50 iPSCs for sequencing with dual index Illumia platform on a HiSeq 4000 sequencing machine. The low input cDNA synthesis and RNA-seq library preparation for ICMs and iPSCs were performed

simultaneously on similar number of cells and pooled together to be sequenced in the same batch to minimize the potential batch effects. The sequencing coverage approximately 50 million reads per RNA-seq sample.

Proteomics sample preparation.

Cells pellets were lysed in 100ul 6M GdmCl, 10mM TCEP, 40mM CAA and 100 mM Tris pH 8.5 buffer. Lysates were incubated at 95 °C for 5 min and briefly sonicated. Samples were boiled for 5min at 95°C and vortexed every 1min, then spinned 5mins + 10mins + 10mins, 12000g, taking supernatant for each step to continue. Protein concentration was measured using the BCA method. Trypsin (modified, from Promega, Madison, WI) was added at a protein to enzyme ratio of 50:1. Samples were incubated overnight at 37 °C. Peptide were added TFA to 1% then cleaned up using an Oasis HLB cartridge (1cc/10mg, Waters). Samples were dried by speed vac and dissolved in 100mM TEAB. Peptides were labeled with TMT 10plex reagent (Thermo Fisher) and combined at equal amounts, then vacuum spun till dry.

Waters 2D liquid chromatography (Waters MClass 2DnLC) was used for peptide separation by reverse phase chromatography at high pH in the first dimension followed by an orthogonal separation at low pH in the second dimension. In the first dimension, the mobile phases were buffer A (20mM ammonium formate at pH10) and buffer B (Acetonitrile). Peptides were separated on an Xbridge 300μm x 5 cm C18 5.0μm column (Waters) using 15 discontinuous step gradients at 2 μl/min. In the second dimension, peptides were loaded to an in-house packed 100μm ID/15μm tip ID x 28cm C18-AQ 1.8μm resin column with buffer A (0.1% formic acid in water). Peptides were separated with a linear gradient from 5% to 40% buffer B (0.1% formic acid in acetonitrile) at a flow rate of 300 nl/min in 112min, 170min and 180 min. The LC system was directly coupled in-line with an Orbitrap Fusion Lumos Tribrid Mass Spectrometer (Thermo Fisher Scientific) via a Thermo nanoelectrospray source. The machine was operated at 1.8-2.2 kV to optimize the nanospray with the ion transfer tube at 275 °C. The mass spectrometer was run in a data dependent mode. The full MS scan was acquired in the Orbitrap mass analyzer with resolution 120,000 at m/z 375-1500 followed by top 20 MS/MS in ion trap. For all sequencing events dynamic exclusion was enabled to fragment peptide once and excluded for 60s.

QUANTIFICATION AND STATISTICAL ANALYSIS

RNA-seq analysis.

The RNAseq analysis was conducted using STAR RNA-seq aligner and RSEM transcript quantification software and the pipeline currently used for the ENCODE project (Dobin et al., 2013, Li and Dewey, 2011, Consortium, 2004). For the downstream analysis DeSEQ2 was used for differential expression analysis (Love et al., 2014). The commonly expressed genes among species were used for quantitative cross-species expression comparisons. The gene-gene interaction networks are based on known interactions on string database(Szklarczyk et al., 2016).

Proteomics data processing and analysis.

The raw data were then processed with the software Proteome Discoverer (Proteome Discoverer, RRID:SCR_014477) (Thermofisher Scientific Inc.). Mass tolerance of 10ppm was used for precursor ion and 0.6 Dalton for fragment ions for the database search. The search included cysteine carbamidomethylation as a fixed modification. Acetylation at protein N-terminus and methionine oxidation were used as variable modifications. Up to two missed cleavages were allowed for trypsin digestion. Only unique peptides with a minimum length of 6 amino acids were considered for protein identification. The false discovery rate (FDR) was set as less than 1%.

Supplementary Material

Refer to Web version on PubMed Central for supplementary material.

Acknowledgment:

Support from gift to Stanford Department of Genetics and Stanford Center for Genomics and Personalized Medicine (SCGPM), California National Primate Research Center (CNPRC) grant P51OD011107, Johns Hopkins University (JHU) grant 5U42OD013117 for the pigtailed macaque colony, and the Southwest National Primate Research Center grant P51OD011133 from the office of Research Infrastructure Programs, National Institute of Health. We would like to thank David Glenn Smith for the continuing support in consultation on nonhuman primate species selection and primate evolutionary biology that apply to the study design and pluripotent stem cell biology. We would like to thank Drs. John Morrison and Jeff Roberts at the CNPRC for their support and facilitating the animal experiments. We also thank Koosha Nassiri Nazif and Mahsa Roodgar for assisting in additional image analysis including the use of KLayout and Matlab and Tuhin K. Guha for assisting in imaging mouse tissue slides. MR is supported by the National Institutes of Health, National Heart Lung Blood Institute (NHLBI) Stanford training grant T32HL120824-6. KVB is supported by the National Institutes of Health, National Human Genome Research Institute (NHGRI) grant K99HG010362. VKB is supported by a grant CA160997. K.M.L. is a Packard Foundation Fellow, Pew Scholar, Human Frontier Science Program Young Investigator, Baxter Foundation Faculty Scholar, and The Anthony DiGenova Endowed Faculty Scholar.

References

ARDEHALI R, INLAY MA, ALI SR, TANG C, DRUKKER M & WEISSMAN IL 2011. Overexpression of BCL2 enhances survival of human embryonic stem cells during stress and obviates the requirement for serum factors. Proceedings of the National Academy of Sciences, 108, 3282–3287.

BAN H, NISHISHITA N, FUSAKI N, TABATA T, SAEKI K, SHIKAMURA M, TAKADA N, INOUE M, HASEGAWA M & KAWAMATA S 2011. Efficient generation of transgene-free human induced pluripotent stem cells (iPSCs) by temperature-sensitive Sendai virus vectors. Proceedings of the National Academy of Sciences, 108, 14234–14239.

BENDALL SC, STEWART MH, MENENDEZ P, GEORGE D, VIJAYARAGAVAN K, WERBOWETSKI-OGILVIE T, RAMOS-MEJIA V, ROULEAU A, YANG J & BOSSÉ M 2007. IGF and FGF cooperatively establish the regulatory stem cell niche of pluripotent human cells in vitro. Nature, 448, 1015–1021. [PubMed: 17625568]

BLAUWKAMP TA, NIGAM S, ARDEHALI R, WEISSMAN IL & NUSSE R 2012. Endogenous Wnt signalling in human embryonic stem cells generates an equilibrium of distinct lineage-specified progenitors. Nature communications, 3, 1–10.

BOROVIAK T, STIRPARO GG, DIETMANN S, HERNANDO-HERRAEZ I, MOHAMMED H, REIK W, SMITH A, SASAKI E, NICHOLS J & BERTONE P 2018. Single cell transcriptome analysis of human, marmoset and mouse embryos reveals common and divergent features of preimplantation development. Development, 145, dev167833. [PubMed: 30413530]

BRONS IGM, SMITHERS LE, TROTTER MW, RUGG-GUNN P, SUN B, DE SOUSA LOPES SMC, HOWLETT SK, CLARKSON A, AHRLUND-RICHTER L & PEDERSEN RA 2007. Derivation

of pluripotent epiblast stem cells from mammalian embryos. Nature, 448, 191–195. [PubMed: 17597762]

BROWN CJ, DUNBAR VG & SHAFER DA 1986. A comparison of the karyotypes of six species of the genus Macaca and a species of the genus Cercocebus. Folia Primatologica, 46, 164–172.

CHEN G, GULBRANSON DR, HOU Z, BOLIN JM, RUOTTI V, PROBASCO MD, SMUGA-OTTO K, HOWDEN SE, DIOL NR & PROPSON NE 2011a. Chemically defined conditions for human iPSC derivation and culture. Nature methods, 8, 424. [PubMed: 21478862]

CHEN G, GULBRANSON DR, HOU Z, BOLIN JM, RUOTTI V, PROBASCO MD, SMUGA-OTTO K, HOWDEN SE, DIOL NR, PROPSON NE, WAGNER R, LEE GO, ANTOSIEWICZ-BOURGET J, TENG JM & THOMSON JA 2011b. Chemically defined conditions for human iPSC derivation and culture. Nat Methods, 8, 424–9. [PubMed: 21478862]

CHEN G, GULBRANSON DR, HOU Z, BOLIN JM, RUOTTI V, PROBASCO MD, SMUGA-OTTO K, HOWDEN SE, DIOL NR, PROPSON NE, WAGNER R, LEE GO, ANTOSIEWICZ-BOURGET J, TENG JMC & THOMSON JA 2011c. Chemically defined conditions for human iPSC derivation and culture. Nature Methods, 8, 424–9. [PubMed: 21478862]

CONSORTIUM, E. P. 2004. The ENCODE (ENCyclopedia of DNA elements) project. Science, 306, 636–640. [PubMed: 15499007]

DAILEY R & NEILL J 1981. Seasonal variation in reproductive hormones of rhesus monkeys: anovulatory and short luteal phase menstrual cycles. Biology of reproduction, 25, 560–567. [PubMed: 6796143]

DE PRADA JKN & VANDEVOORT CA 2008. Growth hormone and in vitro maturation of rhesus macaque oocytes and subsequent embryo development. Journal of assisted reproduction and genetics, 25, 145–158. [PubMed: 18278582]

DOBIN A, DAVIS CA, SCHLESINGER F, DRENKOW J, ZALESKI C, JHA S, BATUT P, CHAISSON M & GINGERAS TR 2013. STAR: ultrafast universal RNA-seq aligner. Bioinformatics, 29, 15–21. [PubMed: 23104886]

DUNN S-J, MARTELLO G, YORDANOV B, EMMOTT S & SMITH A 2014. Defining an essential transcription factor program for naive pluripotency. Science, 344, 1156–1160. [PubMed: 24904165]

FANG R, LIU K, ZHAO Y, LI H, ZHU D, DU Y, XIANG C, LI X, LIU H & MIAO Z 2014. Generation of naive induced pluripotent stem cells from rhesus monkey fibroblasts. Cell stem cell, 15, 488–497. [PubMed: 25280221]

FUSAKI N, BAN H, NISHIYAMA A, SAEKI K & HASEGAWA M 2009. Efficient induction of transgene-free human pluripotent stem cells using a vector based on Sendai virus, an RNA virus that does not integrate into the host genome. Proceedings of the Japan Academy, Series B, 85, 348–362.

GADUE P, HUBER TL, PADDISON PJ & KELLER GM 2006. Wnt and TGF-β signaling are required for the induction of an in vitro model of primitive streak formation using embryonic stem cells. Proceedings of the National Academy of Sciences, 103, 16806–16811.

GAFNI O, WEINBERGER L, MANSOUR AA, MANOR YS, CHOMSKY E, BEN-YOSEF D, KALMA Y, VIUKOV S, MAZA I, ZVIRAN A, RAIS Y, SHIPONY Z, MUKAMEL Z, KRUPALNIK V, ZERBIB M, GEULA S, CASPI I, SCHNEIR D, SHWARTZ T, GILAD S, AMANN-ZALCENSTEIN D, BENJAMIN S, AMIT I, TANAY A, MASSARWA R, NOVERSHTERN N & HANNA JH 2013. Derivation of novel human ground state naive pluripotent stem cells. Nature, 504, 282–6. [PubMed: 24172903]

GIBBS RA, ROGERS J, KATZE MG, BUMGARNER R, WEINSTOCK GM, MARDIS ER, REMINGTON KA, STRAUSBERG RL, VENTER JC & WILSON RK 2007. Evolutionary and biomedical insights from the rhesus macaque genome. science, 316, 222–234. [PubMed: 17431167]

HALL J, GUO G, WRAY J, EYRES I, NICHOLS J, GROTEWOLD L, MORFOPOULOU S, HUMPHREYS P, MANSFIELD W, WALKER R, TOMLINSON S & SMITH A 2009. Oct4 and LIF/Stat3 additively induce Krüppel factors to sustain embryonic stem cell self-renewal. Cell Stem Cell, 5, 597–609. [PubMed: 19951688]

HERMERÉN G 2015. Ethical considerations in chimera research. Development, 142, 3–5. [PubMed: 25516962]

HUANG S-MA, MISHINA YM, LIU S, CHEUNG A, STEGMEIER F, MICHAUD GA, CHARLAT O, WIELLETTE E, ZHANG Y, WIESSNER S, HILD M, SHI X, WILSON CJ, MICKANIN C, MYER V, FAZAL A, TOMLINSON R, SERLUCA F, SHAO W, CHENG H, SHULTZ M, RAU C, SCHIRLE M, SCHLEGL J, GHIDELLI S, FAWELL S, LU C, CURTIS D, KIRSCHNER MW, LENGAUER C, FINAN PM, TALLARICO JA, BOUWMEESTER T, PORTER JA, BAUER A & CONG F 2009. Tankyrase inhibition stabilizes axin and antagonizes Wnt signalling. Nature, 461, 614–20. [PubMed: 19759537]

JØRGENSEN FG, HOBOLTH A, HORNSHØJ H, BENDIXEN C, FREDHOLM M & SCHIERUP MH 2005. Comparative analysis of protein coding sequences from human, mouse and the domesticated pig. BMC biology, 3, 2. [PubMed: 15679890]

KING M-C & WILSON AC 1975. Evolution at two levels in humans and chimpanzees. Science, 188, 107–116. [PubMed: 1090005]

LI B & DEWEY CN 2011. RSEM: accurate transcript quantification from RNA-Seq data with or without a reference genome. Bmc Bioinformatics, 12.

LIAN X, HSIAO C, WILSON G, ZHU K, HAZELTINE LB, AZARIN SM, RAVAL KK, ZHANG J, KAMP TJ & PALECEK SP 2012. Robust cardiomyocyte differentiation from human pluripotent stem cells via temporal modulation of canonical Wnt signaling. Proceedings of the National Academy of Sciences, 109, E1848–E1857.

LIAN X, ZHANG J, AZARIN SM, ZHU K, HAZELTINE LB, BAO X, HSIAO C, KAMP TJ & PALECEK SP 2013. Directed cardiomyocyte differentiation from human pluripotent stem cells by modulating Wnt/β-catenin signaling under fully defined conditions. Nature protocols, 8, 162. [PubMed: 23257984]

LIU T, LI J, YU L, SUN H-X, LI J, DONG G, HU Y, LI Y, SHEN Y & WU J 2021. Cross-species single-cell transcriptomic analysis reveals pre-gastrulation developmental differences among pigs, monkeys, and humans. Cell discovery, 7, 1–17. [PubMed: 33390590]

LOH KM & LIM B 2015. Equilibrium established. Nature, 521, 299. [PubMed: 25993958]

LOVE MI, HUBER W & ANDERS S 2014. Moderated estimation of fold change and dispersion for RNA-seq data with DESeq2. Genome biology, 15, 550. [PubMed: 25516281]

MARTELLO G, BERTONE P & SMITH A 2013. Identification of the missing pluripotency mediator downstream of leukaemia inhibitory factor. The EMBO journal, 32, 2561–2574. [PubMed: 23942233]

MARTELLO G & SMITH A 2014. The nature of embryonic stem cells. Annual review of cell and developmental biology, 30, 647–675.

MARTELLO G, SUGIMOTO T, DIAMANTI E, JOSHI A, HANNAH R, OHTSUKA S, GÖTTGENS B, NIWA H & SMITH A 2012. Esrrb is a pivotal target of the Gsk3/Tcf3 axis regulating embryonic stem cell self-renewal. Cell stem cell, 11, 491–504. [PubMed: 23040478]

MASAKI H, KATO-ITOH M, TAKAHASHI Y, UMINO A, SATO H, ITO K, YANAGIDA A, NISHIMURA T, YAMAGUCHI T, HIRABAYASHI M, ERA T, LOH KM, WU SM, WEISSMAN IL & NAKAUCHI H 2016. Inhibition of Apoptosis Overcomes Stage-Related Compatibility Barriers to Chimera Formation in Mouse Embryos. Cell Stem Cell, 19, 587–592. [PubMed: 27814480]

MITALIPOV S, KUO HC, BYRNE J, CLEPPER L, MEISNER L, JOHNSON J, ZEIER R & WOLF D 2006. Isolation and characterization of novel rhesus monkey embryonic stem cell lines. Stem Cells, 24, 2177–86. [PubMed: 16741224]

MOSSAHEBI-MOHAMMADI M, QUAN M, ZHANG J-S & LI X 2020. FGF signaling pathway: a key regulator of stem cell pluripotency. Frontiers in cell and developmental biology, 8, 79. [PubMed: 32133359]

NAKAI R, OHNUKI M, KUROKI K, ITO H, HIRAI H, KITAJIMA R, FUJIMOTO T, NAKAGAWA M, ENARD W & IMAMURA M 2018. Derivation of induced pluripotent stem cells in Japanese macaque (Macaca fuscata). Scientific reports, 8, 1–9. [PubMed: 29311619]

NAVARA CS, HORNECKER J, GROW D, CHAUDHARI S, HORNSBY PJ, ICHIDA JK, EGGAN K & MCCARREY JR 2013. Derivation of induced pluripotent stem cells from the baboon: a

nonhuman primate model for preclinical testing of stem cell therapies. Cellular Reprogramming (Formerly" Cloning and Stem Cells"), 15, 495–502.

NEI M, XU P & GLAZKO G 2001. Estimation of divergence times from multiprotein sequences for a few mammalian species and several distantly related organisms. Proceedings of the National Academy of Sciences, 98, 2497–2502.

NIWA H, OGAWA K, SHIMOSATO D & ADACHI K 2009. A parallel circuit of LIF signalling pathways maintains pluripotency of mouse ES cells. Nature, 460, 118–122. [PubMed: 19571885]

O'BRIEN SJ, MENNINGER JC & NASH WG 2006. Atlas of mammalian chromosomes, John Wiley & Sons.

OHMINE S, DIETZ AB, DEEDS MC, HARTJES KA, MILLER DR, THATAVA T, SAKUMA T, KUDVA YC & IKEDA Y 2011. Induced pluripotent stem cells from GMP-grade hematopoietic progenitor cells and mononuclear myeloid cells. Stem cell research & therapy, 2, 46. [PubMed: 22088171]

QIU D, YE S, RUIZ B, ZHOU X, LIU D, ZHANG Q & YING Q-L 2015. Klf2 and Tfcp2l1, Two Wnt/β-Catenin Targets, Act Synergistically to Induce and Maintain Naive Pluripotency. Stem cell reports, 5, 314–322. [PubMed: 26321140]

RIESEN J, MEYER R & WOLF R 1971. The effect of season on occurrence of ovulation in the rhesus monkey. Biology of reproduction, 5, 111–114. [PubMed: 5000818]

ROMERO IG, PAVLOVIC BJ, HERNANDO-HERRAEZ I, ZHOU X, WARD MC, BANOVICH NE, KAGAN CL, BURNETT JE, HUANG CH & MITRANO A 2015. A panel of induced pluripotent stem cells from chimpanzees: a resource for comparative functional genomics. Elife, 4, e07103. [PubMed: 26102527]

SAVATIER P, OSTEIL P & TAM PP 2017. Pluripotency of embryo-derived stem cells from rodents, lagomorphs, and primates: Slippery slope, terrace and cliff. Stem cell research, 19, 104–112. [PubMed: 28126658]

SCHRAMM RD, PAPROCKI AM & VANDEVOORT CA 2003. Causes of developmental failure of in-vitro matured rhesus monkey oocytes: impairments in embryonic genome activation. Human Reproduction, 18, 826–833. [PubMed: 12660279]

SOKOL SY 2011. Maintaining embryonic stem cell pluripotency with Wnt signaling. Development, 138, 4341–50. [PubMed: 21903672]

STIRPARO GG, BOROVIAK T, GUO G, NICHOLS J, SMITH A & BERTONE P 2018. Integrated analysis of single-cell embryo data yields a unified transcriptome signature for the human pre-implantation epiblast. Development, 145.

SUCHY F & NAKAUCHI H 2017. Lessons from interspecies mammalian chimeras. Annual review of cell and developmental biology, 33, 203–217.

SZKLARCZYK D, GABLE AL, LYON D, JUNGE A, WYDER S, HUERTA-CEPAS J, SIMONOVIC M, DONCHEVA NT, MORRIS JH & BORK P 2019. STRING v11: protein–protein association networks with increased coverage, supporting functional discovery in genome-wide experimental datasets. Nucleic acids research, 47, D607–D613. [PubMed: 30476243]

SZKLARCZYK D, MORRIS JH, COOK H, KUHN M, WYDER S, SIMONOVIC M, SANTOS A, DONCHEVA NT, ROTH A & BORK P 2016. The STRING database in 2017: quality-controlled protein–protein association networks, made broadly accessible. Nucleic acids research, gkw937.

TACHIBANA M, SPARMAN M, RAMSEY C, MA H, LEE H-S, PENEDO MCT & MITALIPOV S 2012. Generation of chimeric rhesus monkeys. Cell, 148, 285–295. [PubMed: 22225614]

TAI C-I & YING Q-L 2013. Gbx2, a LIF/Stat3 target, promotes reprogramming to and retention of the pluripotent ground state. Journal of cell science, 126, 1093–1098. [PubMed: 23345404]

TAKAHASHI K, TANABE K, OHNUKI M, NARITA M, ICHISAKA T, TOMODA K & YAMANAKA S 2007. Induction of pluripotent stem cells from adult human fibroblasts by defined factors. Cell, 131, 861–72. [PubMed: 18035408]

TAKASHIMA Y, GUO G, LOOS R, NICHOLS J, FICZ G, KRUEGER F, OXLEY D, SANTOS F, CLARKE J, MANSFIELD W, REIK W, BERTONE P & SMITH A 2014. Resetting Transcription Factor Control Circuitry toward Ground-State Pluripotency in Human. Cell, 158, 1254–1269. [PubMed: 25215486]

TAN T, WU J, SI C, DAI S, ZHANG Y, SUN N, ZHANG E, SHAO H, SI W & YANG P 2021. Chimeric contribution of human extended pluripotent stem cells to monkey embryos ex vivo. Cell, 184, 2020–2032. e14. [PubMed: 33861963]

TESAR PJ, CHENOWETH JG, BROOK FA, DAVIES TJ, EVANS EP, MACK DL, GARDNER RL & MCKAY RD 2007. New cell lines from mouse epiblast share defining features with human embryonic stem cells. Nature, 448, 196–199. [PubMed: 17597760]

THEUNISSEN TW, POWELL BE, WANG H, MITALIPOVA M, FADDAH DA, REDDY J, FAN ZP, MAETZEL D, GANZ K, SHI L, LUNGJANGWA T, IMSOONTHORNRUKSA S, STELZER Y, RANGARAJAN S, D'ALESSIO A, ZHANG J, GAO Q, DAWLATY MM, YOUNG RA, GRAY NS & JAENISCH R 2014. Systematic Identification of Culture Conditions for Induction and Maintenance of Naive Human Pluripotency. Cell Stem Cell, 15, 524–526. [PubMed: 28903030]

VALLIER L, ALEXANDER M & PEDERSEN RA 2005. Activin/Nodal and FGF pathways cooperate to maintain pluripotency of human embryonic stem cells. Journal of cell science, 118, 4495–4509. [PubMed: 16179608]

VANDEVOORT CA, MTANGO NR, LATHAM KE & STEWART DR 2011. Primate preimplantation embryo is a target for relaxin during early pregnancy. Fertil Steril, 96, 203–7. [PubMed: 21645893]

VANDEVOORT CA, MTANGO NR, LEE YS, SMITH GW & LATHAM KE 2009. Differential effects of follistatin on nonhuman primate oocyte maturation and pre-implantation embryo development in vitro. Biology of reproduction, 81, 1139–1146. [PubMed: 19641179]

VANDEVOORT CA & TARANTAL AF 1991. The macaque model for in vitro fertilization: superovulation techniques and ultrasound-guided follicular aspiration. J Med Primatol, 20, 110–6. [PubMed: 1895329]

VANDEVOORT CA & TARANTAL AF 2001. Recombinant human gonadotropins for macaque superovulation: repeated stimulations and post-treatment pregnancies. J Med Primatol, 30, 304–7. [PubMed: 11990529]

WANG X, LI T, CUI T, YU D, LIU C, JIANG L, FENG G, WANG L, FU R & ZHANG X 2018. Human embryonic stem cells contribute to embryonic and extraembryonic lineages in mouse embryos upon inhibition of apoptosis. Cell research, 28, 126. [PubMed: 29099092]

WU J, GREELY HT, JAENISCH R, NAKAUCHI H, ROSSANT J & BELMONTE JCI 2016. Stem cells and interspecies chimaeras. Nature, 540, 51–59. [PubMed: 27905428]

WU J, OKAMURA D, LI M, SUZUKI K, LUO C, MA L, HE Y, LI Z, BENNER C & TAMURA I 2015. An alternative pluripotent state confers interspecies chimaeric competency. Nature, 521, 316. [PubMed: 25945737]

WU J, PLATERO-LUENGO A, SAKURAI M, SUGAWARA A, GIL MA, YAMAUCHI T, SUZUKI K, BOGLIOTTI YS, CUELLO C, MORALES VALENCIA M, OKUMURA D, LUO J, VILARINO M, PARRILLA I, SOTO DA, MARTINEZ CA, HISHIDA T, SANCHEZ-BAUTISTA S, MARTINEZ-MARTINEZ ML, WANG H, NOHALEZ A, AIZAWA E, MARTINEZ-REDONDO P, OCAMPO A, REDDY P, ROCA J, MAGA EA, ESTEBAN CR, BERGGREN WT, NUNEZ DELICADO E, LAJARA J, GUILLEN I, GUILLEN P, CAMPISTOL JM, MARTINEZ EA, ROSS PJ & IZPISUA BELMONTE JC 2017. Interspecies Chimerism with Mammalian Pluripotent Stem Cells. Cell, 168, 473–486 e15. [PubMed: 28129541]

WU Y, ZHANG Y, MISHRA A, TARDIF SD & HORNSBY PJ 2010. Generation of induced pluripotent stem cells from newborn marmoset skin fibroblasts. Stem Cell Research, 4, 180–188. [PubMed: 20363201]

YAMANE T, DYLLA SJ, MUIJTJENS M & WEISSMAN IL 2005. Enforced Bcl-2 expression overrides serum and feeder cell requirements for mouse embryonic stem cell self-renewal. Proceedings of the National Academy of Sciences, 102, 3312–3317.

YANG J, VAN OOSTEN AL, THEUNISSEN TW, GUO G, SILVA JC & SMITH A 2010. Stat3 activation is limiting for reprogramming to ground state pluripotency. Cell stem cell, 7, 319–328. [PubMed: 20804969]

YEO J-C, JIANG J, TAN Z-Y, YIM G-R, NG J-H, GÖKE J, KRAUS P, LIANG H, GONZALES KAU, CHONG H-C, TAN C-P, LIM Y-S, TAN N-S, LUFKIN T & NG H-H 2014. Klf2 Is an Essential Factor that Sustains Ground State Pluripotency. Cell Stem Cell, 14, 864–72. [PubMed: 24905170]

YURI S, FUJIMURA S, NIMURA K, TAKEDA N, TOYOOKA Y, FUJIMURA YI, ABURATANI H, URA K, KOSEKI H & NIWA H 2009. Sall4 is essential for stabilization, but not for pluripotency, of embryonic stem cells by repressing aberrant trophectoderm gene expression. Stem cells, 27, 796–805. [PubMed: 19350679]

ZHONG B, TROBRIDGE GD, ZHANG X, WATTS KL, RAMAKRISHNAN A, WOHLFAHRT M, ADAIR JE & KIEM H-P 2011. Efficient generation of nonhuman primate induced pluripotent stem cells. Stem cells and development, 20, 795–807. [PubMed: 21058905]

- Improved culture of chimp and pig-tailed macaque iPSCs by inhibiting WNT signaling
- Endogenous high expression of *BCL2* in the rhesus inner cell mass
- Expression of *BCL2* enhances proliferation of chimp iPSCs in rhesus early embryo
- Co-culture of chimp and human iPSCs can differentiate into integrated cardiomyocytes

Roodgar et al. demonstrate an improved culture of chimpanzee and pig-tailed macaque iPSCs. They show high expression of endogenous BCL2 in rhesus macaque ICM. Through over expression of BCL2 in chimpanzee iPSCs they generate primate cross-species pre-implantation embryos composed of chimpanzee iPSCs and rhesus pre-implantation embryos.

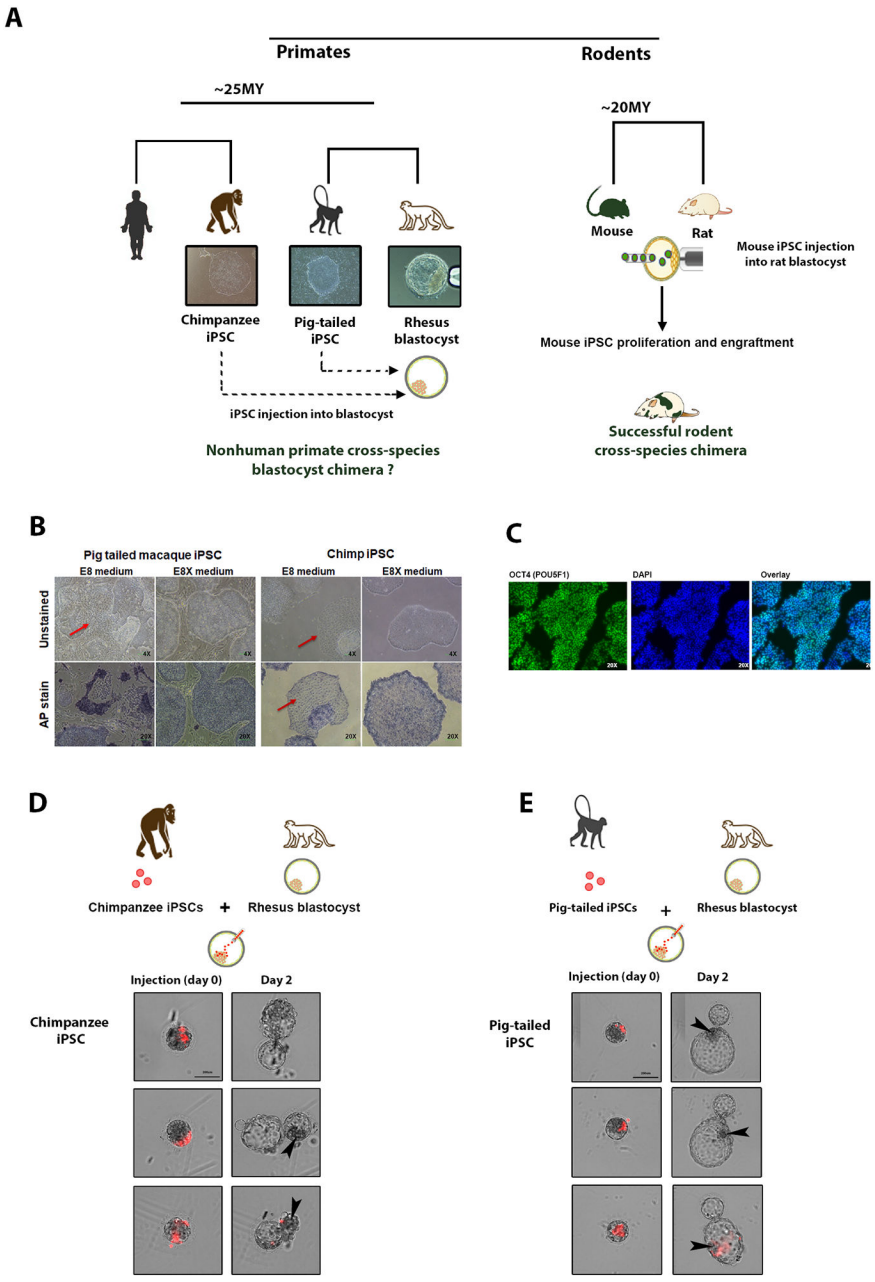

Figure 1. Survival and proliferation of chimpanzee and pig-tailed macaque donor iPSCs in rhesus macaque host embryos

A) Phylogenetic tree comparing evolutionary distance across human, chimpanzee, pig-tailed macaque, and rhesus macaque primate species, as well as rodent species. Schematic figure demonstrates previously successful cross-species chimera using rodent iPSCs (mouse) and rodent blastocysts (rat), however whether primate iPSCs are capable of in forming cross-species chimera remains unknown. Representative examples of optimized chimpanzee-derived iPSCs and pig-tailed macaque iPSCs maintained in E8X media, and rhesus macaque host embryo blastocyst are shown.

B) Morphology of pig-tailed macaque iPSCs on MEF in E8 or E8X media (left) and chimpanzee colonies on iMatrix in E8 or E8X media (right). Red arrows indicate the differentiating cells surrounding the iPSC colonies in the media E8 media, little-to-no differentiating cells were observed in E8X medium.

C) POU5F1 staining of the iPSCs before injection into the mouse testis for teratoma formation.

D) 3 Representative imaging examples of tdTomato (tdT) red fluorescent protein expression as a marker for Chimpanzee iPSCs maintained in E8X media and injected to rhesus blastocysts at day 0 (left) and day 2 (right). Success and failure of iPSC survival was categorically defined by the presence and absence of tdT, respectively. Chimpanzee iPSCs survive and proliferate near rhesus ICM at low efficiency (success rate = 1 out of 3 embryos (33.3%)). Black arrow indicating the inner cell mass.

E) 3 Representative imaging examples of tdTomato (tdT) red fluorescent protein expression as a marker for pig-tailed macaque iPSCs maintained in E8X media and injected to rhesus blastocysts at day 0 (left) and day 2 (right). Success and failure of iPSC survival was categorically defined by the presence and absence of tdT, respectively. Pig-tailed macaque iPSCs survive and proliferate near rhesus ICM at low efficiency (success rate = 6 out of 11 embryos (54.5%)). Black arrow indicating the inner cell mass.

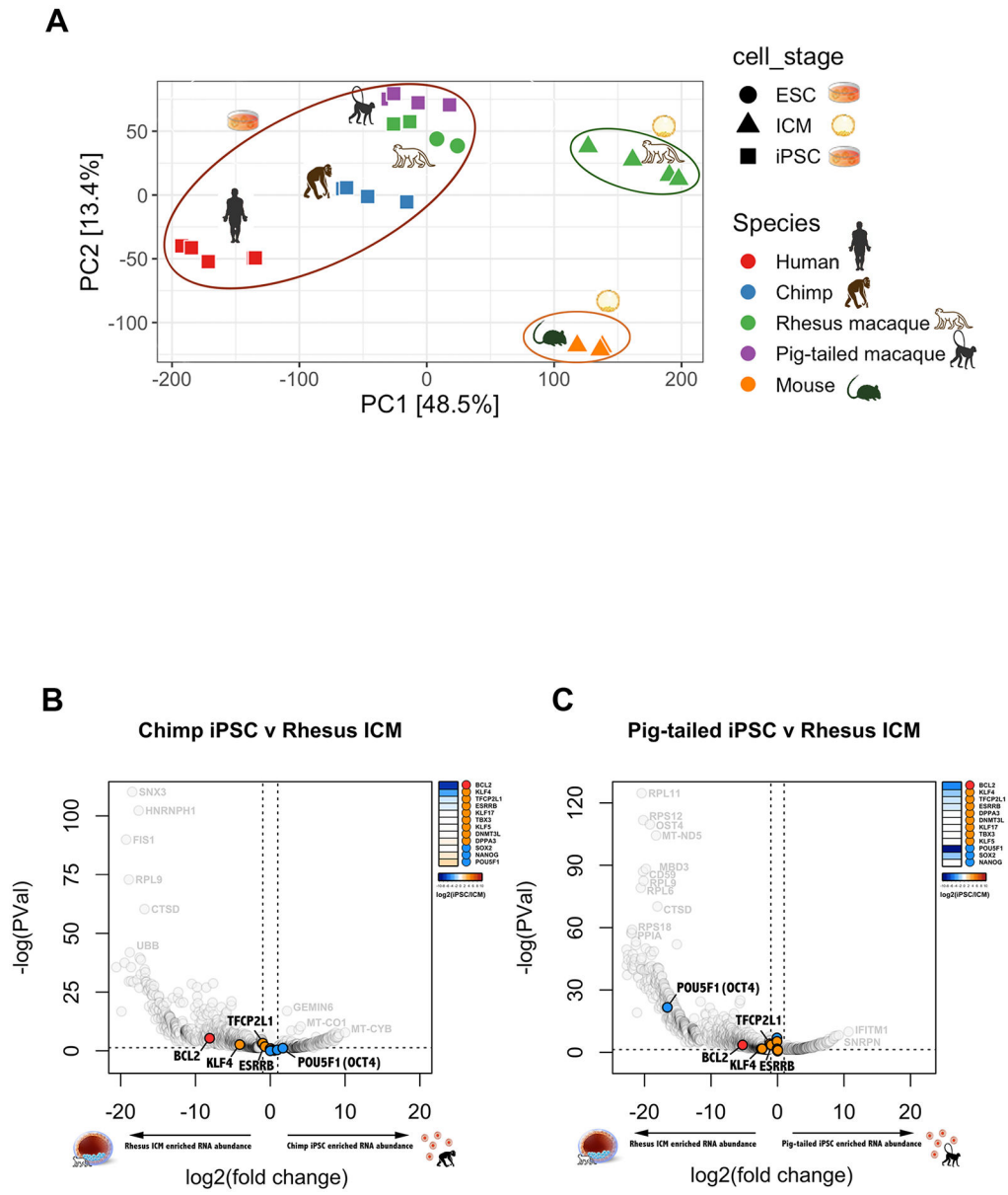

Figure 2. Analysis of primate iPSCs and rhesus macaque ICM transcriptome profiles reveals higher expression of *BCL2* in rhesus macaque ICM compared to chimpanzee and pig-tailed macaque iPSCs.

A) Principal component analysis (PCA) of transcript abundance patterns cluster by cell types (or stages) indicating separation of ICMs and pluripotent stem cells (PSCs) along the first principal component (PC1) in the gene expression data (PC1= 48.5% separates ICM from all PSCs).

B) Volcano plot comparing transcriptome of chimpanzee iPSCs with rhesus ICM, blue dots indicate pluripotency related genes

C) Volcano plot comparing transcriptome of pig-tailed iPSCs with rhesus ICM, blue dots indicate pluripotency related genes

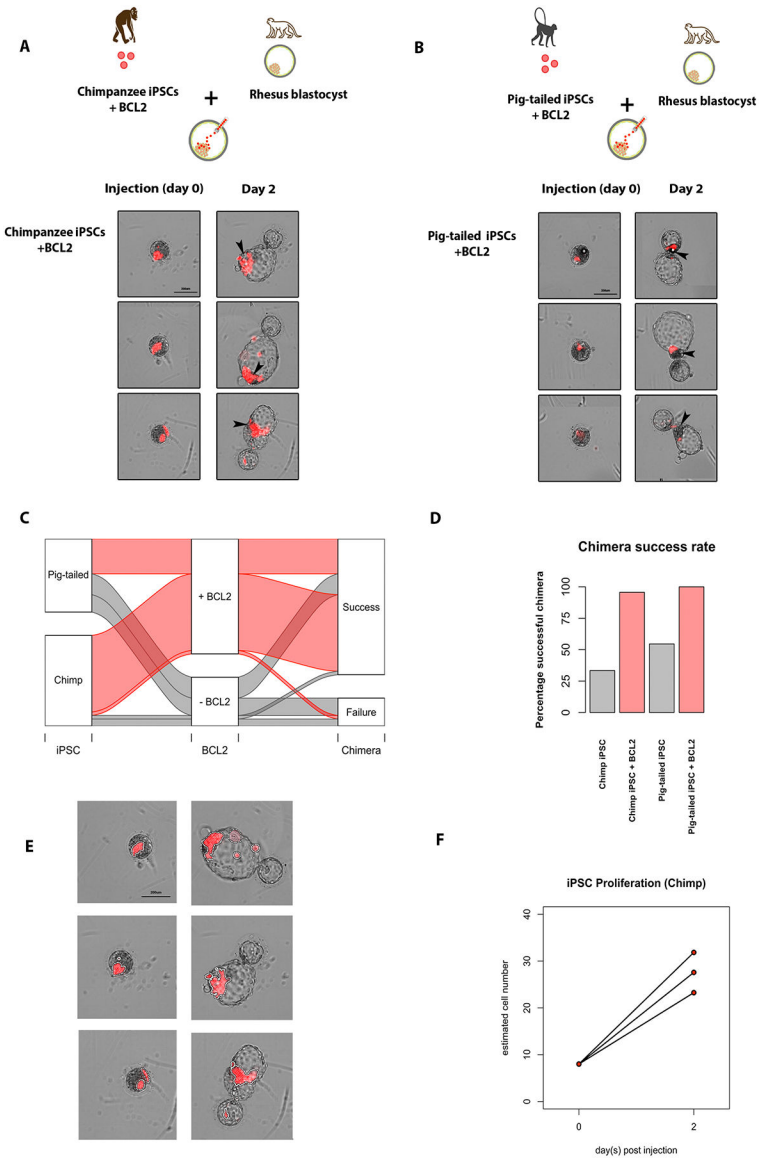

Figure 3. *BCL2* overexpression in chimpanzee and pig-tailed macaque donor iPSCs improves the success rate of *ex vivo* survival and proliferation of chimpanzee and pig-tailed macaque donor iPSCs in rhesus macaque host embryos.

A) Overexpression of *BCL2* in chimpanzee iPSCs facilitates survival and proliferation of chimpanzee iPSCs near rhesus macaque ICM. 3 Representative imaging examples of tdTomato (tdT) red fluorescent protein expression as a marker for ectopic *BCL2*-expressing chimpanzee iPSCs maintained in E8X media and injected to rhesus blastocysts at day 0 (left) and day 2 (right). Success and failure of iPSC survival was categorically defined by the presence and absence of tdT, respectively. chimpanzee iPSCs survive and proliferate near rhesus ICM at low efficiency (success rate = 22 out of 23 embryos (95.7%)). Black arrow indicating the inner cell mass.

B) Overexpression of *BCL2* in pig-tailed macaque iPSCs facilitates survival and proliferation of pig-tailed macaque iPSCs near rhesus macaque ICM. 3 Representative imaging examples of tdTomato (tdT) red fluorescent protein expression as a marker for

ectopic *BCL2*-expressing pig-tailed macaque iPSCs maintained in E8X media and injected to rhesus blastocysts at day 0 (left) and day 2 (right). Success and failure of iPSC survival was categorically defined by the presence and absence of tdT, respectively. chimpanzee iPSCs survive and proliferate near rhesus ICM at low efficiency (success rate = 10 out of 10 embryos (100%)). Black arrow indicating the inner cell mass.

C) Visualization of success and failure of donor iPSCs survival in rhesus macaque host embryos and either pig-tailed macaque or chimpanzee iPSC donor cells, +/− ectopic *BCL2* expression via alluvial plot.

D) Visualization of success rate of donor iPSCs survival in rhesus macaque host embryos and either pig-tailed macaque or chimpanzee iPSC donor cells, +/− ectopic *BCL2* expression (pig-tailed macaque +/− *BCL2* success rate = 100% and 54.5%, respectively; chimpanzee macaque +/− *BCL2* success rate = 95.7% and 33.3%, respectively).

E) Survival and proliferation of ectopic *BCL2*-expressing chimpanzee iPSCs maintained in E8X media and injected to rhesus blastocysts at day 0 (left) and two days after injection (right). Survival and proliferation of chimpanzee is determined by the expansion of the red area of tdTomato (tdT) red fluorescent protein expression as a marker for chimpanzee iPSCs.

F) iPSCs proliferation and indirect estimation of the number proliferated iPSCs 2 days post infection via measurement of the expanded red-fluorescent pixel area.

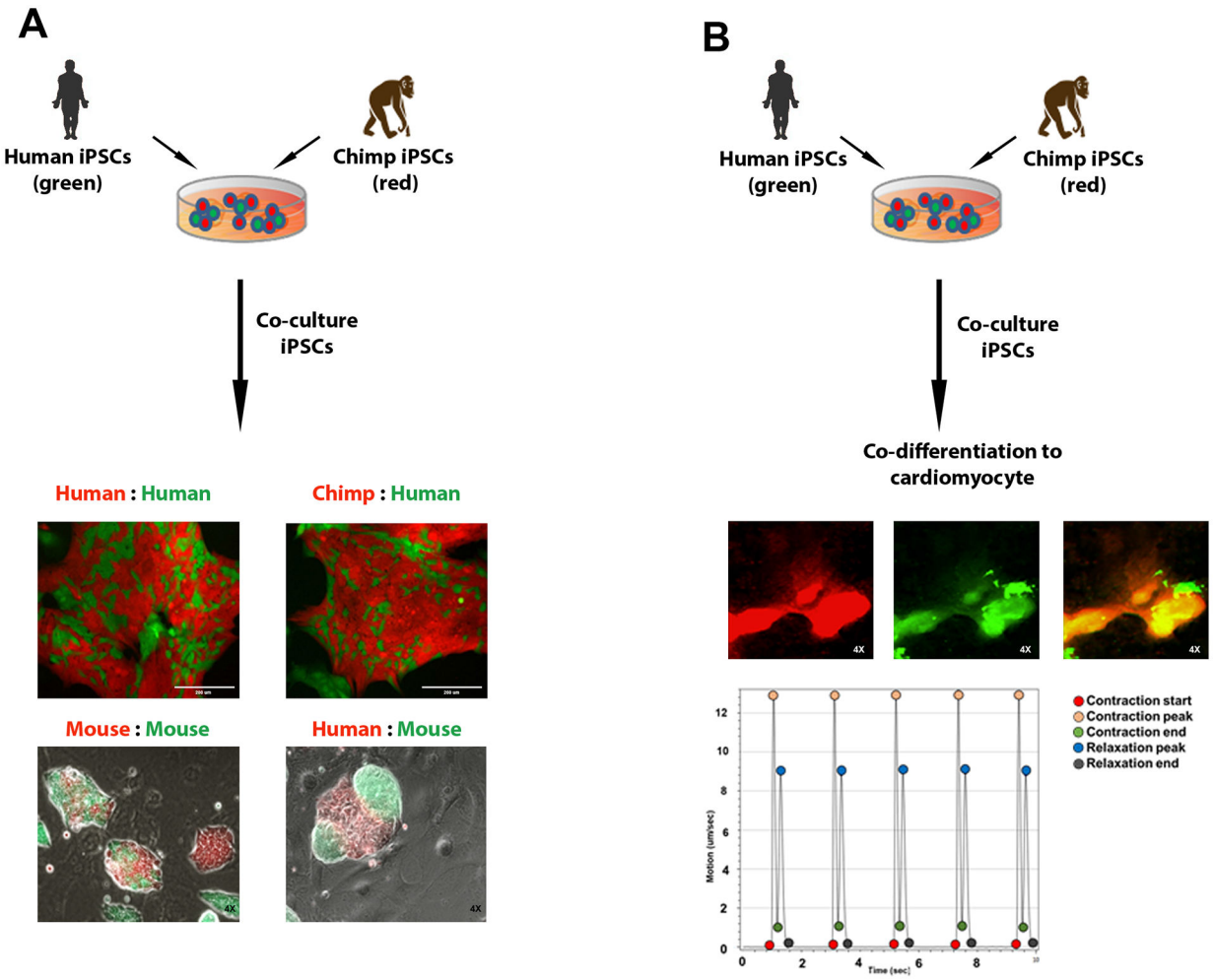

Figure 4. Chimpanzee iPSCs serve as an appropriate surrogate for human iPSCs.

A) Schematic figure of co-culture experiment of ~20,000 human and ~20,000 of chimpanzee iPSCs (top panel). Bottom panel indicating four pictures of various iPSCs co-culture experiments from human-human iPSCs co-culture (top-left) and human-chimp iPSCs (top-right). Human and chimpanzee iPSCs mix and integrate homogenously without forming segregated colonies. Co-culture of mouse-mouse iPSCs form mixed and homogenously integrated colonies (bottom-left). Human and mouse iPSCs form separate and segregated colonies (bottom-right).

B) Schematic figure of co-culture experiment of ~20,000 human and ~20,000 of chimpanzee iPSCs (top panel) for differentiation into cardiomyocytes. Bottom panel showing cardiomyocyte layers differentiated from the co-culture mixture of chimpanzee and human iPSCs. The tdTomato-fluorescent labeled beating chimpanzee iPSCs (red, left) and the human GFP-fluorescent labeled beating cardiomyocyte (green, middle) and the overlay image of the mixed cardiomyocytes from the mixture of chimpanzee and human iPSCs (Supplementary videos 2 and 3). Electrocardiogram of cardiomyocyte derived from the mixture of human and chimpanzee iPSCs indicating contraction and relaxation start, peak, and end (right).

Table 1.

The summary of the number of both chimp and pig-tailed with or without *BCL2* into rhesus. Red fluorescent *BCL2*-expressing (B) Chimpanzee or (C) Pig-tailed macaque iPSCs survive, proliferate and localize near rhesus ICM 2 days post injection imaged through in vitro culture.

Recipient Embryo	iPSC donor species	Total Embryos	Developed Embryos	Chimerism
Rhesus	Chimp, no BCL2	12	4 (33.0%)	1/3 (33.0%)
Rhesus	**Chimp with BCL2**	**46**	**23 (50.0%)**	**22/23 (95.6%)**
Rhesus	Pig-tailed, no BCL2	20	11 (55.0%)	6/11 (54.5%)
Rhesus	**Pig-tailed with BCL2**	**20**	**10 (50.0%)**	**10/10 (100.0%)**
Rhesus	All	98	48 (48.9%)	39

KEY RESOURCES TABLE

REAGENT or RESOURCE	SOURCE	IDENTIFIER
Antibodies		
POU5F1	Santa Cruz Biotechnology	Cat # sc-8628
NR2F1	Abcam	Cat # ab41858
PAX3	Santa Cruz Biotechnology	Cat # sc-4916
p75	Promega	Cat # G323A
Alexa Fluor 488	ThermoFisher	Cat # A-11055
Alexa Fluor 647	ThermoFisher	Cat # A-21447
POU5F1	Cell Signaling Technology	Cat # 2750S
NANOG	Cell Signaling Technology	Cat # 3580S
Biological samples		
Chimpanzee PBMCs recovered from intravenous whole blood collection	This paper	N/A
Pig-tailed macaque PBMCs recovered from intravenous whole blood collection	This paper	N/A
Rhesus macaque embryos generated via IVF	This paper	N/A
Chemicals, peptides, and recombinant proteins		
WNT inhibitor (XAV939)	TOCRIS	Cat # 3748
Thiazovivine (TZV)	TOCRIS	Cat # 3845
Essential 8 medium	Gibco	Cat # A1517001
Essential 6 Medium	Gibco	Cat # A1516401
bFGF	ThermoFisher	Cat # 13256029
Stem Span SFEM	Stem Cell Technologies	Cat # 09600
Stem Span Erythroid Expansion Supplement	Stem Cell Technologies	Cat # 02692
Recombinant RNAse inhibitor	TaKaRa	Cat # 2313A
Critical commercial assays		
RNeasy Mini Ki	QIAGEN	Cat # 74104
SMART-Seq Ultra Low input RNA-sequencing kit	TaKaRa	Cat # 634891
Agilent High-Sensitivity DNA Reagent	Agilent	Cat # 5067-4627
Deposited data		
Rhesus macaque inner cell mass, iPSCs and ESCs RNA-sequencing data	This paper	GSE155443
Chimpanzee iPSCs RNA-sequencing data	This paper	GSE155443
Pig-tailed macaque iPSCs RNA-sequencing data	This paper	GSE155443
Mouse inner cell mass RNA-sequencing data	This paper	GSE155443
Rhesus macaque inner cell mass, iPSCs and ESCs RNA-sequencing data	This paper	GSE155443
Experimental models: Cell lines		
Chimpanzee: induced pluripotent stem cells	This paper	N/A

REAGENT or RESOURCE	SOURCE	IDENTIFIER
Pig-tailed macaque: induced pluripotent stem cells	This paper	N/A
Rhesus macaque: induced pluripotent stem cells	This paper	N/A
Rhesus macaque: Embryonic stem cells - (ORMES)-6	Oregon National Primate Research Center	Mitalipov et al. 2006https://doi.org/10.1634/stemcells.2006-0125
Experimental models: Organisms/strains		
Chimpanzee: induced pluripotent stem cells	This paper	N/A
Pig-tailed macaque: induced pluripotent stem cells	This paper	N/A
Rhesus macaque: induced pluripotent stem cells	This paper	N/A
Rhesus macaque: Embryonic stem cells - (ORMES)-6	Oregon National Primate Research Center	Mitalipov et al. 2006https://doi.org/10.1634/stemcells.2006-0125
Oligonucleotides		
pou5f1 (Oct3/4)	Applied Biosystems	Rh02843075_g1
hBCL2	ThermoFisher	This paper
td-Tomato	ThermoFisher	This paper
RhKLF4	Applied Biosystems	Rh02847953_m1
RhESRRB	Applied Biosystems	Rh02848660_m1
Recombinant DNA		
CS-TRE-BCL2-PRE-Ubc-rtTA-IRES2-NeoR	Masaki et al. 2016	Masaki et al. 2016
piggyback CAG-tdTomato	Masaki et al. 2016	Masaki et al. 2016
Software and algorithms		
STAR	N/A	https://github.com/alexdobin/STAR
FlowJo	FlowJo	https://www.flowjo.com
Prism 8	GraphPad	N/A
R package STRINGdb	Bioconductor	https://www.string-db.org
ImageJ	NIH	https://imagej.nih.gov/ij/
RSEM	https://github.com/deweylab/RSEM	http://deweylab.biostat.wisc.edu
KLayout	N/A	https://www.klayout.de/
DESeq2 R package	Bioconductor	10.18129/B9.bioc.DESeq2
Other		
BZ-9000 microscope	Keyence	http://www.keyence.com
Agilent 2100 Bioanalyzer instrument	Agilent	https://www.agilent.com/
Revolve microscope	Echo	http://www.dicover-echo.com